

# FEASIBILITY STUDY FOR A SINGLE-SHOT 3D ELECTRON BUNCH CHARGE DISTRIBUTION MONITOR WITH A POLARIZED PROBE LASER AT SPring-8 PHOTOINJECTOR

Y. Okayasu, H. Tomizawa, S. Matsubara,

A. Mizuno, H. Dewa, H. Hanaki, K. Yanagida, S. Suzuki and T. Taniuchi,  
JASRI, 1-1-1 Kouto, Sayo-cho, Sayo-gun, Hyogo 679-5198, Japan

A. Maekawa and M. Uesaka, Nuclear Professional School, University of Tokyo  
2-22 Shirakata-Shirane, Tokai, Naka, Ibaraki 319-1188, Japan

T. Ishikawa, RIKEN, 1-1-1 Kouto, Sayo-cho, Sayo-gun, Hyogo 679-5198, Japan

## Abstract

In linac-based ultra high brightness light sources, It is necessary to characterize the light emission bunch-by-bunch for high precision experiments. Monitoring three dimensional bunch shape (charge density distribution) in real time with high resolution is an essential key for precise optimization of an X-ray FEL's beam. Therefore, we developed a single-shot and non-destructive three bunch charge distribution monitor and successfully promoted a feasibility test with a 200 ps linearly chirped probe laser pulse and two ZnTe crystals. It is based on Electro-Optic (EO) simultaneous and multiple sampling with a manner of spectral decoding. In order to realize precise measurements of both transverse and longitudinal charge distribution simultaneously, at least eight EO crystals surrounding the electron bunch axis and radial polarized and hollow-shaped probe laser are required. Numerical calculation for the hollow-shaped laser propagation along the realistic monitoring system is conducted and shows that radial polarization at the designed EO crystals position in an assembling holder can be fine adjusted.

## INTRODUCTION

SACLA accelerator (SPring-8 Angstrom Compact free electron Laser) has been completed its construction at the SPring-8 site and the beam commissioning has been proceeded since the end of 2010. A slice emittance of  $0.7 - 1.0 \pi$  mm-mrad and a peak current of 4.4 kA are required for its standard operation, thus the electron bunches are compressed to 30 fs (FWHM) through three staged bunch compression [1]. In order to measure the temporal distribution of such 8 GeV electron bunches, the measurement with an RF deflector [2, 3] is the most reliable method at present, and there is a plan to install it in SACLA [3]. It is, however, destructive measurement, and therefore cannot be used in operation for SASE (Self-Amplified Spontaneous Emission) generation. Hence, another diagnostics system with non-destructive measurement is required for beam tuning to generate stable SASE radiation for user experiments.

According to these above situation, we introduce a three dimensional electron bunch shape monitor (3D-BSM), which is based on the Electro-Optic (EO) sampling bunch duration techniques [4], described in Fig. 1. The 3D-BSM

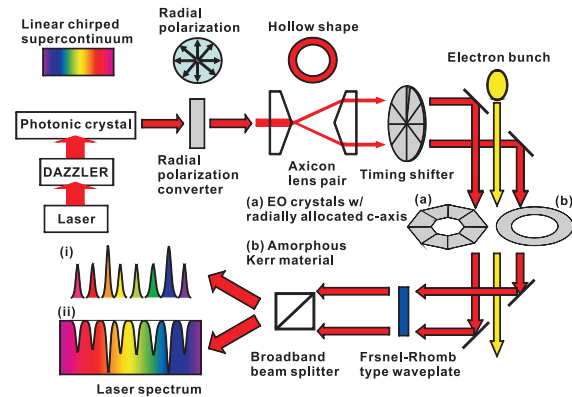


Figure 1: A schematic view of the 3D-BSM configuration.

is consisted of three detector sections. The center of mass of the electron bunch and its incident angle are defined with amorphous materials at both end (Fig. 1(b)), which enables background free detection due to the Kerr effect. The 3D charge distribution of the electron bunch is monitored by EO crystals (Pockels effect, Fig. 1(a)) which are allocated in the center of two doughnut-shaped amorphous detectors. Each detector is based on EO-sampling with a manner of spectral decoding, which enables single-shot measurements using linear chirped laser pulses. The primary function of the monitor can be divided into transverse and longitudinal detection. For starters, eight EO crystals surround the beam axis azimuthally, and a linear chirped probe laser with hollow shape propagates through each crystal. Both the EO crystal axis and the polarization axis of the probe laser should be radially distributed as well as the Coulomb field of the electron bunches. The signal intensity encoded at each EO crystal depends on the field strength at each point. Therefore, the signal intensity changes as the transverse charge distribution of the electron bunches becomes asymmetric. In order to detect the intensity modulation of each signal in real time, the laser pulse spectra should be a rectangular intensity distribution with a linear chirp in phase. Further details of the principle of transverse and energy chirp detection are discussed in Ref. [5].

In the longitudinal detection, a very high temporal resolution of several tens of femtoseconds in FWHM is required for SACLA. In the spectral decoding, one of the main factors limiting temporal resolution ( $T_{res}$ ) is the

bandwidth of a probe laser. It is expressed as  $T_{res} \sim \sqrt{\tau_o \tau_c}$  where  $\tau_o$  is the pulse width of the Fourier transform limited pulse of the probe laser and  $\tau_c$  is the pulse width of the probe laser with a linear chirp [6]. With a 400 fs spectral bandwidth and a broadband square spectrum ( $\geq 400$  nm at 800 nm of a central wavelength), the resolution is estimated to be less than 30 fs.

Other considerable factors, which limit the temporal resolution, are the following spectral transmission characteristics of EO materials, 1) absorption in THz range, 2) velocity mismatch inside the materials between a THz pulse (the Coulomb field) and a probe laser pulse and 3) dispersion of EO materials in a spectral range of a broadband probe laser. As far as using ZnTe or GaP for the bunch duration measurements, which are generally adopted as inorganic EO crystals, their temporal resolutions are limited to  $\sim 120$  fs (FWHM) at present. It is because ZnTe and GaP have their phonon absorption at around 5 and 11 THz, respectively [7]. Thus, the Coulomb field is distorted as propagate in such crystals. However, in order to achieve 30 fs temporal resolution, EO materials should be transparent up to 30 THz [10]. DAST is one of the candidates which is organic and used as the broadband THz source (2 - 31.5 THz, a sharp and narrow absorption due to optical photon resonance at 1.1 THz) [8]. It is also expected to be effective for the ultra short bunch shape measurements. DAST is transparent in the spectral range of more than 600 nm. This is the reason we set the spectral range of 600 - 1100 nm for the probe laser generation.

As discussed above, a broadband linear chirped laser pulse with rectangular-shaped intensity spectrum is required for our 3D-BSM. The spectral range required for the system is 600 - 1100 nm and we are preparing such a broadband probe laser with a photonic crystal fiber and a NOPA amplifier [11]. In addition, the probe laser profile should be hollow with a radial polarization over the whole spectral region. In this paper, we report the feasibility demonstration for the 3D-BSM both in aspects of experiments and numerical calculations.

### EXPERIMENTS

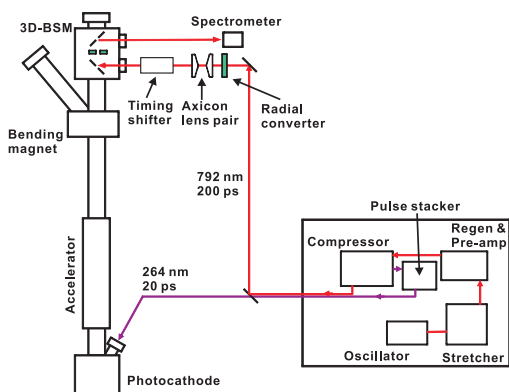


Figure 2: A schematic experimental apparatus with a prototype of the 3D-BSM chamber.

We performed 3D-BSM feasibility experiments for a prototype monitor chamber in the advanced photocathode RF gun test facility, SPring-8. Fig. 2 shows the experimental setup and a laser distribution with an automatic alignment system in the facility [12]. In the 3D-BSM chamber, two 1 mm thick ZnTe crystals were installed diagonally. Both crystals were placed at 4 mm from the electron beam axis. The birefringence induced by the transverse electric field of 200 ps (FWHM) duration of the electron beam bunch was probed 4 ~ 5 mm from the axis by a hollow laser beam with a 1 mm ring width. In the 3D-BSM, Pockels EO crystals are installed in the number of  $2^n$  surrounding the electron beam axis azimuthally for simultaneous transverse detection. This feasibility experiment is the simplest case,  $n = 1$ . The probe laser is a hollow laser with linear polarization. Note that a radial polarization is required when we probe more than eight crystals ( $n \geq 3$ ) simultaneously. For starter, a single EO signal was measured

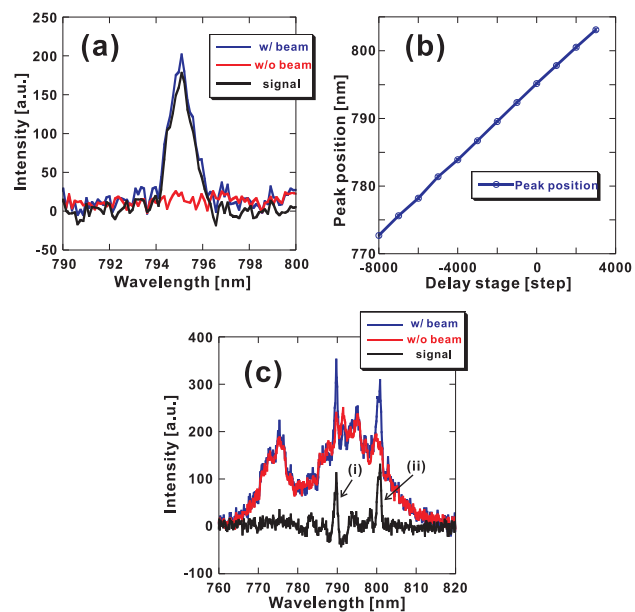


Figure 3: Experimental results of EO signal at the photocathode RF phase of  $80^\circ$  (a), chirp linearity of the probe laser (b) and EO signals probed two ZnTe crystals simultaneously (c).

with one of the ZnTe crystals at different RF gun phases ( $50^\circ \leq \theta \leq 100^\circ$ ), and a result at  $\theta = 80^\circ$ , where the signal gain became maximum, is shown in Fig. 3(a). The chirp linearity of this probe hollow laser was measured as a wavelength shift at EO signal peaks while changing the delay time (i.e. arrival time at the EO crystal) of the probe laser pulse. In the delay line, one step of the stage shifts  $8 \mu\text{m}$  ( $\cong 270$  fs). The fitting result of Fig. 3(b) gives a conversion factor of 9.58 ps/nm. During the RF phase scan, we always put an electron bunch on the RF top phase of RF accelerating structures. The measured electron bunch width was 10.8 ps (FWHM) in Fig. 3(a).

Next, double EO signals were measured simultaneously with both ZnTe crystals, and these results are shown in

Fig. 3(c). Each of the EO signals (double peaks with a timing shift of 100 ps) was measured at each EO crystal at the same time.

## NUMERICAL CALCULATIONS

Laser propagation calculations for our designed optical system are proceeded with a generic electromagnetic optical design and analysis program (VirtualLab, LightTrans). First,  $\phi$  2 mm (FWHM) linear polarized Gaussian beam transports  $\sim 20$  m air space, then propagate through  $\phi$  50.8 mm fused silica axicon lens pair. Distance between two axicon lenses in a pair is adjusted to be 35 mm in order to generate  $\phi$  8 mm hollow-shaped laser at designed EO crystal position. Figure 4(a-c) shows calculated electric

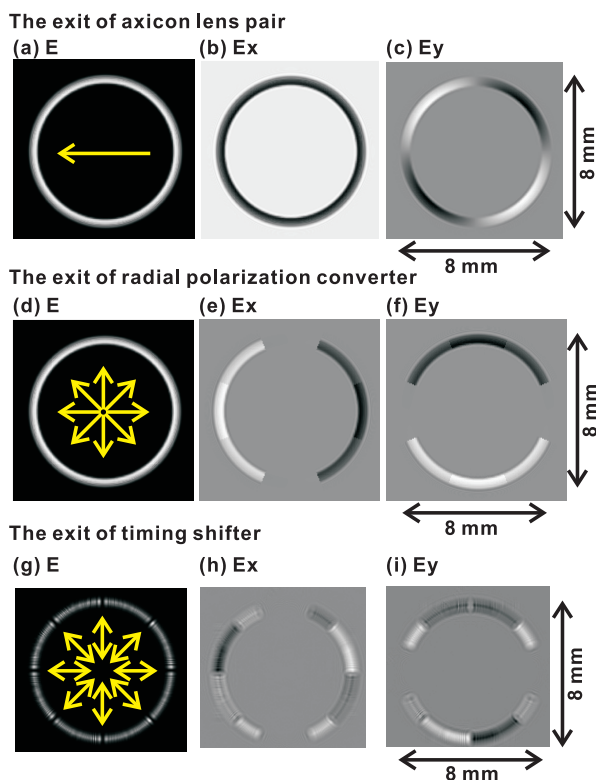


Figure 4: Calculated electric field and polarization at exit of the axicon lens pair (a) - (c), the radial polarization converter (an eight segmented waveplate) (d) - (f) and the timing shifter (g) - (i). In each figure, single or double-headed arrows distinguish the polarizations are uniform both in the oscillating direction and their pointing phases or only in the former, respectively.

field and polarization distribution at exit of the axicon lens pair. In Fig. 4,  $E$ ,  $E_x$  and  $E_y$  mean summed squared amplitude, transverse and vertical components of the electric field, respectively. In the calculation, the axicon lens pair is configured to make the laser pulse has a 1 mm thick hollow shape with  $\phi$  8 mm outer diameter and has a linear polarization before the radial polarization converter, as shown in Fig. 4(a-c). Then, the laser propagates through the radial polarization converter, polarization of the hollow-

shaped laser is converted from linear to radial, as shown in Fig. 4(d-f). The timing shifter (See Ref. [9] for details) is reconstructed and embedded in the simulation. The electric field and polarization distribution at the exit of the timing shifter are represented in Fig. 4(g-i). It is found that the polarization on the hollow-shaped laser profile keeps radial, however, it is not completely radial, especially in contact region between neighboring glasses. This deformation of the radial polarization is considered to be induced due to stepped wavefront in the boundary region. The wavefront is spirally shifted with 10 - 20 ps steps for this feasibility test. However, such deformed components of the polarization can be excluded by introducing a eight segmented radial polarizer.

By the laser propagation calculation, it is confirmed that the radial polarization generation with hollow-shaped laser is enable which is one of the essential keys to achieve the 3D-BSM.

## SUMMARY

Monitoring ever changing charge distribution of electron bunches by single-shot measurements with high resolution is an essential key for precise characterization of an X-ray FEL's beam. For the above goal, we introduced the 3D-BSM with a manner of spectral decoding. The first experiment with a 200 ps linearly chirped laser pulse and two diagonally allocated ZnTe crystals has been successfully demonstrated. Numerical calculation for the laser propagation is proceeded along our designed 3D-BSM system. Calculation result indicates the radial polarization generation with hollow-shaped laser is feasible, and 30 fs temporal resolution can be realized with our setup as discussed in this paper.

## REFERENCES

- [1] H. Tanaka, T. Hara and K. Togawa, private communications.
- [2] O. H. Altemueller et al., *Rev. Sci. Instr.* **35** 438 (1964).
- [3] H. Ego and Y. Otake, in *Proceedings of EPAC08*, TUPC023, Genova, Italy, p.1098 (2008).
- [4] H. Tomizawa et al., in *Proceedings of FEL2007*, WEPH053, Novosibirsk, Russia, p.472 (2007); H. Tomizawa, Japan Patent Application No: 2007-133046.
- [5] A. Maekawa et al., in *Proceedings of PAC09*, TH6REP045, Vancouver, Canada, p.4054 (2009).
- [6] I. Wilke et al., *Phys. Rev. Lett.* **88** 124801 (2002).
- [7] G. Berden et al., *Phys. Rev. Lett.* **99** 164801 (2007).
- [8] Y. Takahashi et al., *J. Photochem. Photobiol. A : Chem.* **183** 247 (2006).
- [9] H. Tomizawa et al., in *Proceedings of FEL2010*, WEPB20, Malmö, Sweden, p.445 (2010).
- [10] T. Hattori and T. Kobayashi, *Chem. Phys. Lett.* **113**, 230 (1987).
- [11] S. Matsubara et al., in *Proceedings of FEL2009*, TUPC15, Liverpool, UK, p.269 (2009).
- [12] H. Tomizawa, *Rad. Phys. Chem.* (in press).